Advanced Implanted Nanotechnology Microchips From Targeted Individual Made Of Diamonoids - Analysis By Dr. Hildegarde Staninger

Ana Maria Mihalcea, MD, PhD

APPLIED CONSUMER SERVICES, INC.

11890 NW 87th Court , Unit 8, Hialeah Gardens, FL 33018
Phone: (305) 821-1677 Fax: (305) 821-0155 Web:appliedconsumer.com

L/N: **32670**
Date: **10/1/18**

Sample "IHS-9142018-911-A "JL Body Hearts"

OBJECT (FRONT)

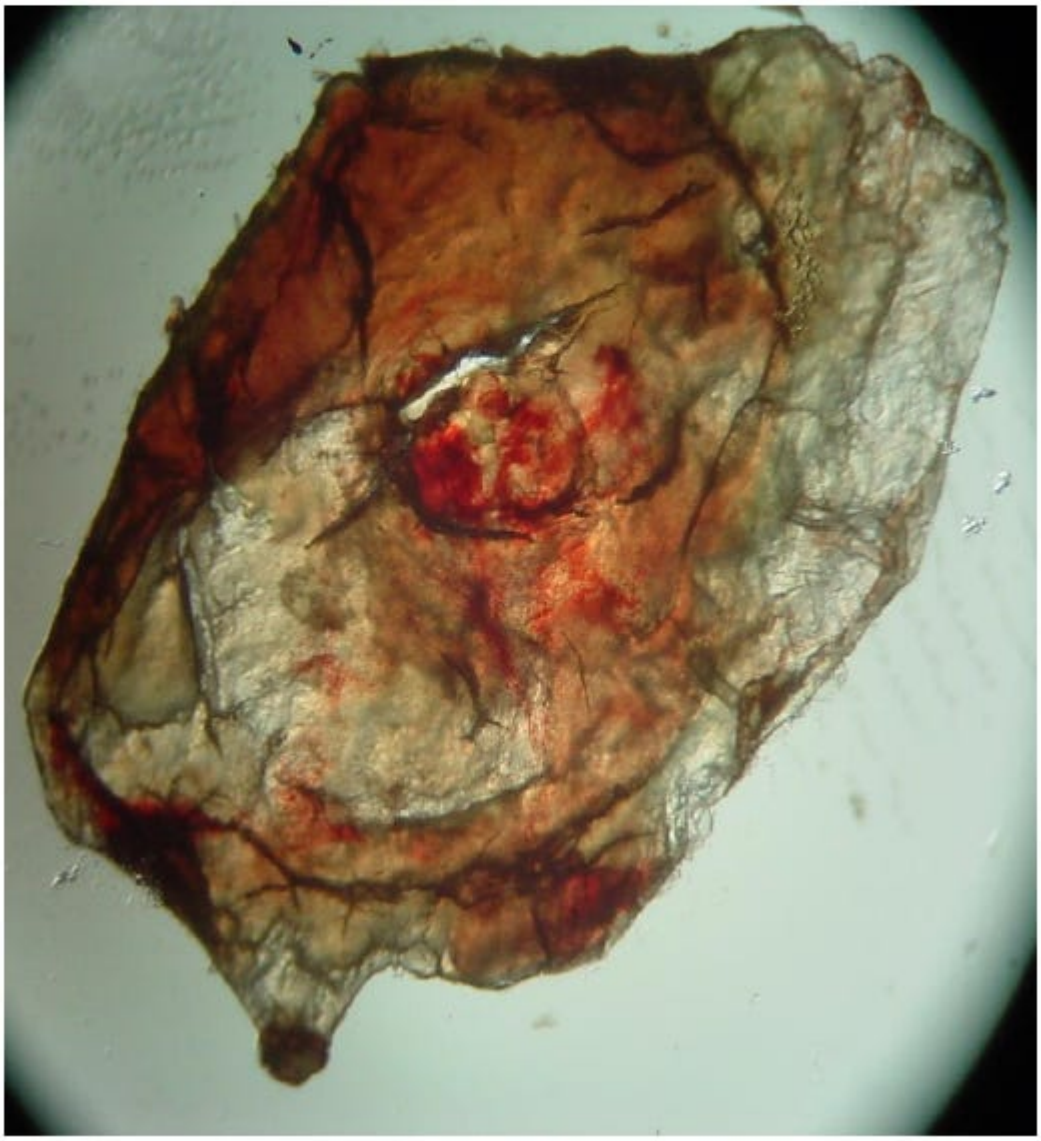

Image: Nano Kirigami HEARTS

Article Authors: Dr Ana Mihalcea and Dr Hildegarde Staninger

Building artificial diamonds is a chaotic process involving trillions of atoms, but conceptual proposals by Robert Freitas and Ralph Merkle contemplate robot arm tips that can remove hydrogen atoms from a source material and deposit them at desired locations in the construction of a molecular machine. In this proposal, the tiny machines are built out of a diamondoid material. In addition to having great strength, the material can be doped with impurities in a precise fashion to create electronic components such as transistors.

-Ray Kurzweil, Google Engineer, Scientific Advisor to US Army, Technocratic Transhumanist in "The Singularity is Near". 2005. p230

Dr. Hildegarde Staninger pioneered the field of science to identify advanced nano materials. Much of this early work was done under Morgellon's research which revealed that the materials were advanced nanotechnology. The work evolved into the evaluation of specimens taken from Targeted Individuals.

We have been discussing this early work which was done 5 or more years ago. The images and research analysis is part of the missing link into the embedded intra body area network systems within the human body - that we now find in COVID19 vaccinated as well as unvaccinated individuals.

The specimen called Body Hearts was analyzed and identified from the field six months prior to the Harvard article by Zhiguang Liu, et. al., "Nano Kirigami with Giant Optical Chirality" was published. These systems have multiple chiral optical antennas and function as a quantum computer platform.

When looking at the specimen called Body Heart you will notice a red crystal material in its center and white leaf like materials around the red crystal. The white leaf material can maintain the frequencies used by the device, which can be as many as 132 signals. The analysis results of FTIR, EDS and SEM are for the red crystal material. If you look at the FTIR Raman Spectroscopy results you will see that the material is composed of synthetic diamonds.

This is the original skin lesion of the Targeted Individual that was surgically excised in 2018 and submitted with full chain of custody for further analysis.

In the images below you can see multiple photographs taken of the specimen.

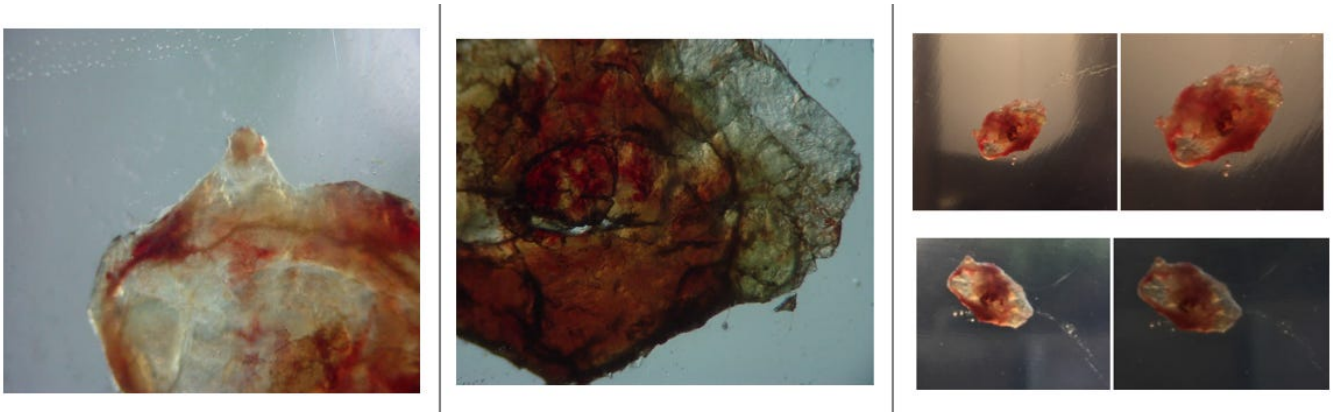

A heart like shape is seen in the center.

APPLIED CONSUMER SERVICES, INC.
11890 NW 87th Court , Unit 8, Hialeah Gardens, FL 33018
Phone: (305) 821-1677 Fax: (305) 821-0155 Web:appliedconsumer.com

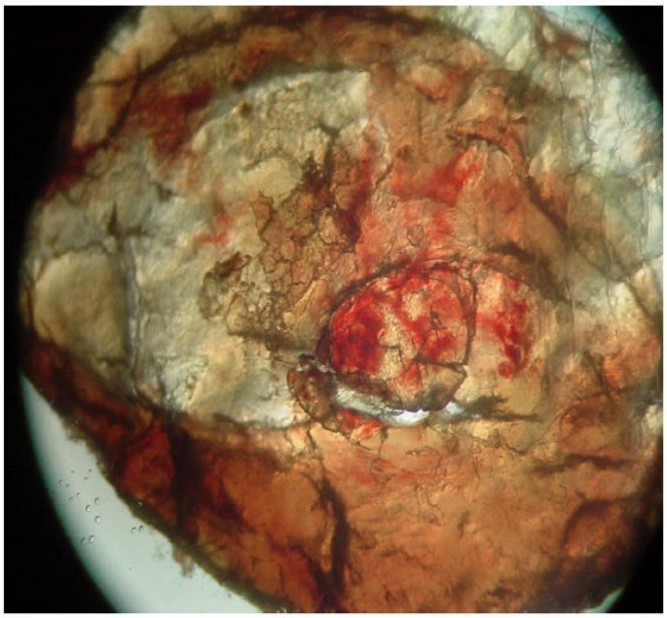

OBJECT (BACK)

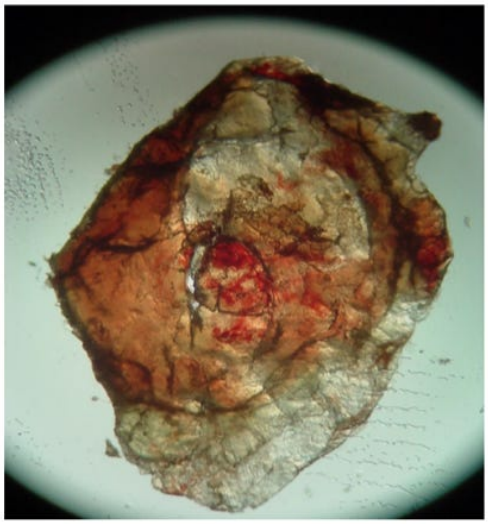

A crystalline material is noted.

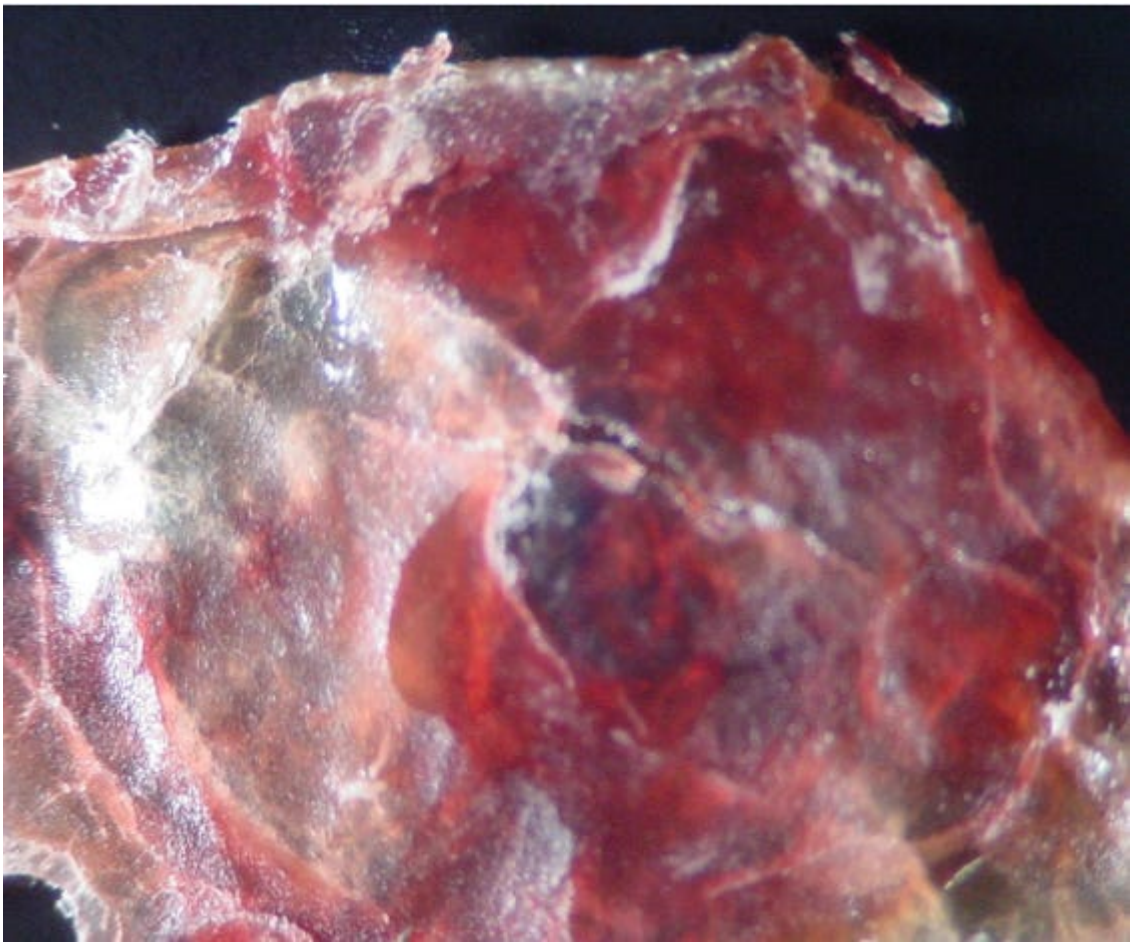

The self assembly process in its completed form reveals a perfect heart shape.

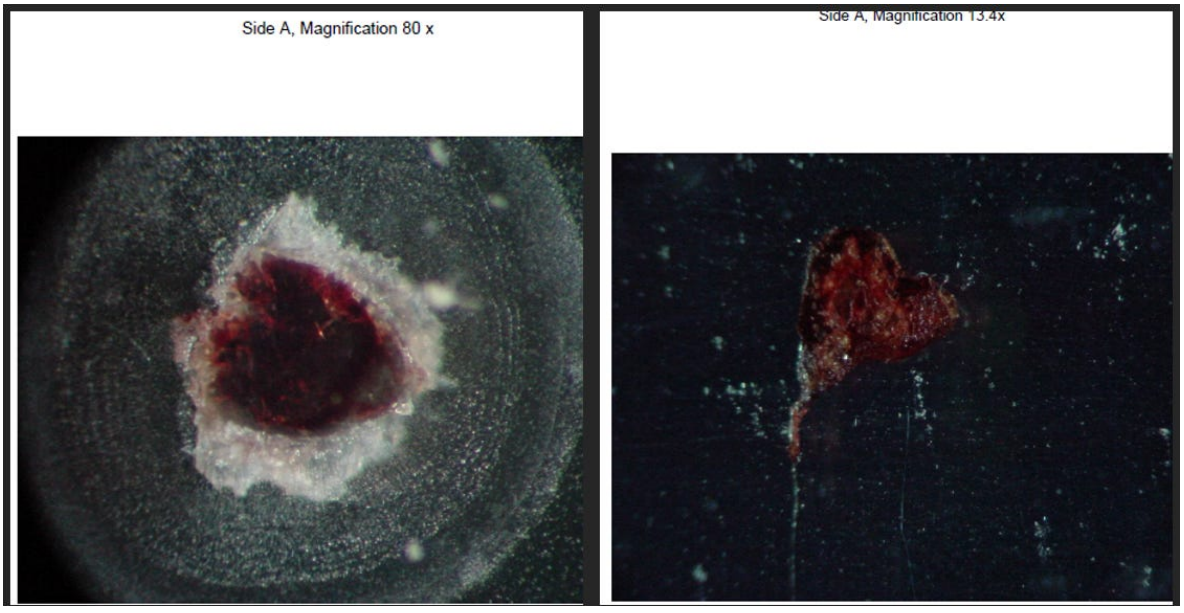

You can see the schematic that shows a wave guide, metal oxides, wire antenna

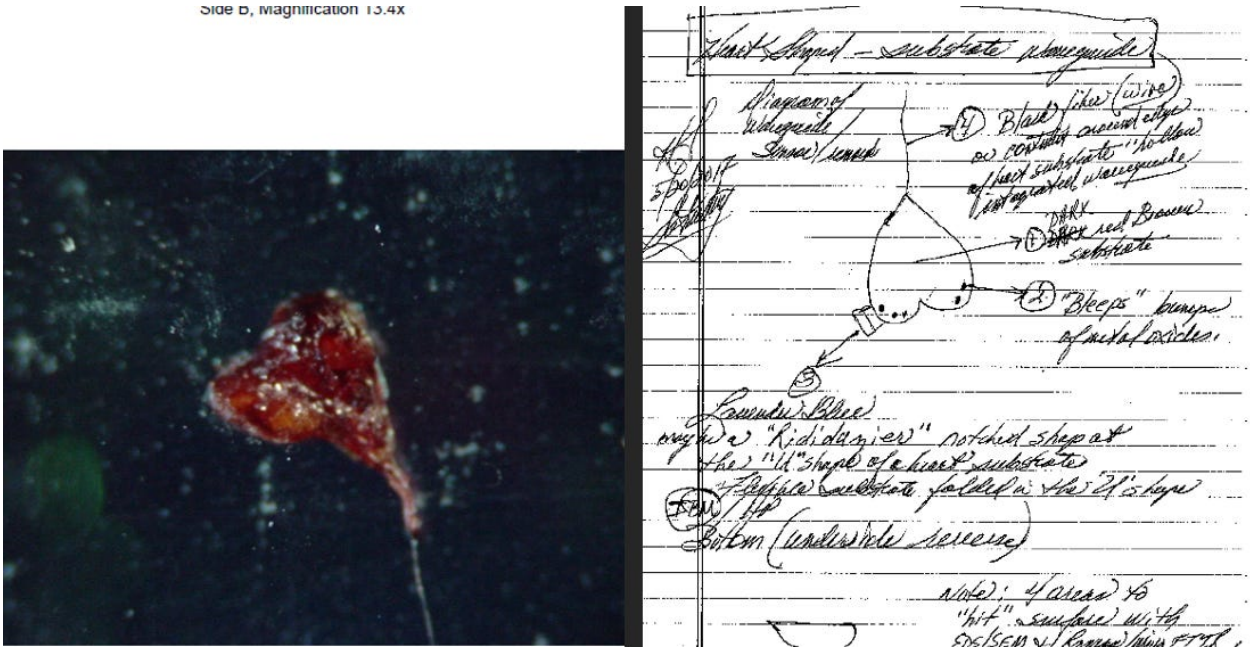

The analysis identified an animal protein as a base.

D/N: 32670

Sample identified as 32670 was submitted for analysis. The sample was carefully selected by cutting them out with a scalpel while viewing under a stereomicroscope. It was placed on a sodium chloride window and analyzed using microscope Fourier transform infrared spectroscopy (FTIR).

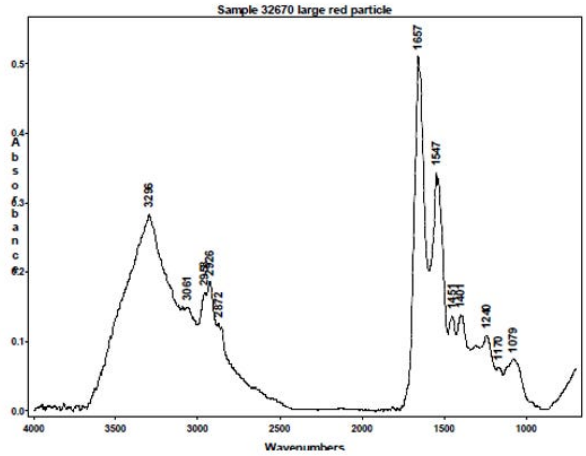

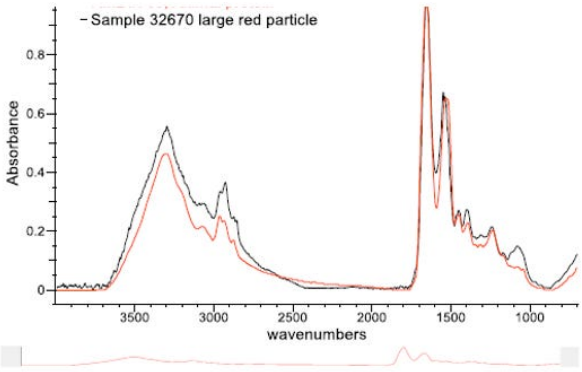

RESULTS AND OBSERVATIONS:

- The sample 32670 large red particle was highly consistent with animal protein.
- Specific assignments for animal protein bands are:

3300 cm-1	NH stretch
3080 cm-1	CNH overtone

Further characterization of its chemical components was done, showing ingredients used for semiconductor microchips. The origin of these chemicals are NOT HUMAN.

Fourier Transform Infrared Spectroscopy (FTIR) Frequencies Identified

LN: 32670 Date: October 6, 2018

Sample identified as 32670 was submitted for analysis. The sample was carefully selected by cutting them out with a scalpel while viewing under a stereomicroscope. It was placed on a sodium chloride window and analyzed using microscope Fourier transform infrared spectroscopy (FTIR). When looking at the image of the specimen the area analyzed was the red crystalline material.

~ 3296 cm^{-1} = In the **polystyrene** spectrum, we see the high frequency carbon-hydrogen (C-H) vibrations at about 3000 cm^{-1}. The low frequency carbon-carbon (C-C) vibrations are at around 800 cm^{-1}. The C-H vibrations have a higher frequency than the C-C vibrations because hydrogen is lighter than carbon.

~3061 cm^{-1} = In the CH region, the highest frequency band is the aromatic CH that appears at 3061 cm^{-1}, the value that is most often quoted for an aromatic CH. Note that this band can move 10–15 cm^{-1} in some modified compounds **Amide II proteins such as amino acids.**

~ 2958 cm^{-1} = **isotatic polybutene** – 1 fibres

~ 2926 cm^{-1}= olefin producing products

~ 2872 cm^{-1} = most intense triplet of **hexane, heptane**, and **polyethylene** on lipid lipid molecule

~ 1657 cm^{-1} = **carotenoids** with strong collagen molecules.

~ 1547 cm^{-1} =

Raman and IR spectra of the free base *p*-sulfonatophenyl and phenyl *meso*-substituted porphyrins [5,10,15,20-tetrakis(4-sulfonatophenyl)porphyrin ($TPPS_4$); 5,10,15-tris(4-sulfonatophenyl)-20-phenyl-porphyrin ($TPPS_3$); 5,10-bis(4-sulfonatophenyl)-15,20-diphenylporphyrin ($TPPS_{2A}$); 5,15-bis(4-sulfonatophenyl)-10,20-diphenylporphyrin ($TPPS_{2O}$); and 5-(4-sulfonatophenyl)-10, 15,20-trisphenylporphyrin ($TPPS_1$)] and their *N*-diprotonated derivatives (porphyrin diacids) were studied.

~ 1451 cm^{-1} =resonant Raman spectra of sub-monolayer PTCDA films on passivated semiconductor surfaces, both before and after annealing the deposited

films at elevated temperatures (350 °C). Independent of the sample treatment, the sub-monolayer Raman spectra

~ 1401 cm^{-1}= microcrystalline films of synthetic diamonds

~ 1240 Cm^{-1} = resonant Raman spectra of sub-monolayer PTCDA films on passivated semiconductor surfaces, both before and after annealing the deposited films at elevated temperatures (350 °C). Independent of the sample treatment, the sub-monolayer Raman spectra.

~ 1159 cm^{-1} = B **carentenoids and astaxandoins.**

~ 1150 cm^{-1} = **The peak near 1150 cm21 in the visible Raman spectra of poor quality chemical-vapor-deposited diamond is often used as the signature of nanocrystalline diamond**. We argue that this peak should not be assigned to nanocrystalline diamond or other sp3-bonded phases

~ 1079 cm^{-1} = presence of **sulfamethoxyazoate and sulfadbenene.**

In the center of the heart shape and pinwheel with optical chirality is seen.

Nano-kirigami with giant optical chirality

The demonstrated nano-kirigami, as well as the exotic 3D nanostructures, could be adopted in broad nanofabrication platforms and could open up new possibilities for the exploration of functional micro-/nanophotonic and mechanical devices.

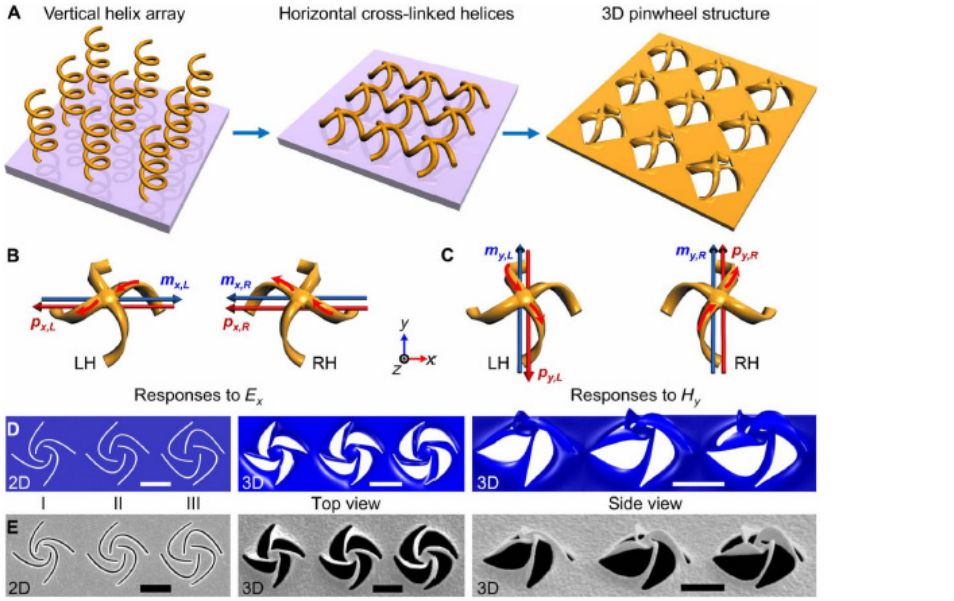

Fig. 3. Functional designs for optical chirality. (**A**) Schematic of vertical helix array, horizontal cross-linked helices, and a 3D pinwheel array [the 3D pinwheel can also be treated as two cross-linked and twisted ohm-shaped circuits (*28*) standing onto a metallic hole array]. (**B** and **C**) Illustration of the responses to the (B) electric field (E_x) and (C) magnetic field (H_y) of incident light for the LH and RH twisted pinwheels, respectively. The direction of induced electric moments $p_{i,j}$ ($i = x$ or y, $j = L$ or R) and magnetic moments $m_{i,j}$ at the center parts is noted by the arrows for LH ($j = L$) and RH ($j = R$) pinwheels, respectively (generalized from the simulated results in fig. S7). (**D**) Numerical designs of three 2D spiral patterns (types I, II, and III), the top view, and side view of the numerically predicted 3D structures, respectively, under the same residual stress distribution. (**E**) SEM images of the fabricated 2D patterns and corresponding 3D pinwheels after global ion irradiation with the same doses, agreeing excellently with the numerical predictions. Scale bars, 1 μm.

Also in 2018 laser-driven electron accelerator so small it could be produced on a silicon chip have been developed.

Paving the way: An accelerator on a microchip

The Accelerator on a Chip International Program (AChIP), funded by the Gordon and Betty Moore Foundation in the U.S., aims to create an electron accelerator on a silicon chip. The fundamental idea is to replace accelerator parts made of metal with glass or silicon, and to use a laser instead of a microwave generator as an energy source. Due to glass's higher electric field load capacity, the acceleration rate can be increased and thus the same amount of energy can be transmitted to the particles within a shorter space, making the accelerator shorter by a factor of approximately 10 than traditional accelerators delivering the same energy.

Silicon nanoantennas have unprescedented ability to control the propagaton of electromagnetic waves.

Silicon nanoantennas turn light around

MOSCOW — Light is rather hard to control, as photons have neither mass nor electric charge. Devices such as nanoantennas can control the propagation of electromagnetic waves, but only to a certain degree.

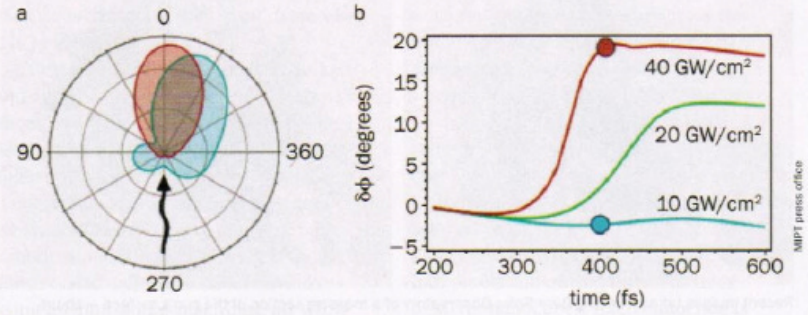

The simulation results of nonlinear light scattering by a nanoantenna of two silicon particles.

A proposed nonlinear optical nanoantenna that can be manipulated will operate at 250 Gbps, shining light, so to speak, on the development of optical computers where information is carried by photons, rather than electrons, greatly increasing the speed of transmitting and processing information.

Physicists from ITMO University in Saint Petersburg, Russia; the Moscow Institute of Physics and Technology (MIPT); and the University of Texas at Austin have developed an unconventional nanoantenna of sorts that can scatter light in a particular direction depending on the intensity of incident radiation.

Using silicon nanoparticles, which gen-

Remember that in optogenetics and biophysics light can control all aspects of the cell cycle and can genetically engineer cellular structures without CRISPR gene editing. Note that in 2017 this nanoantenna control of light was published, but likely achieved in black projects long prior to this date.

Researcher and MIPT postgraduate student Denis Baranov said their nanoantenna is different than existing optical nanoantennas that can control light in a fairly wide range.

"This ability is usually embedded in their geometry and the materials they are made of, so it is not possible to configure these characteristics at any time," said Baranov. "The properties of our nanoantenna, however, can be dynamically modified. When we illuminate it with a weak laser impulse, we get one result, but with a strong impulse, the outcome is completely different."

Carotenoids, which were found in the chemical analysis, have very specific specific electronic resonance spectra and can be used to analyze very specific biologial systems.

[Carotenoids—Their Resonance Raman Spectra and How They Can Be Helpful in Characterizing a Number of Biological Systems]

Carotenoids serve multiple uses in biological systems ranging from visual pigments to antioxidants. Because the resonance Raman spectrum varies with subtle chemical changes on the functional side groups, the spectra of carotenoids have been used for identification and characterization…The *carotenoids* are a class of highly colored materials whose electronic absorption is derived from the polyene backbone of the molecule.

Polystyrene is a polymer that also has been found as a stealth nanoparticle in the Moderna patent of COVID19 bioweapons. Polybutene is an organic polymer, which we will discuss further in a follow up substack, as I have described 2 years ago that butanal is a chemical component of both the COVD19 bioweapon and the filaments sprayed via Geoengineering, showing a chemical overlap and further evidence of the global satanic technocratic transhumanist agenda.

Many people want to jam the signals of the microchips, but they do not understand that one of these microchips as presented here can emit up to 132 frequencies, and if one is jammed, the system simply jumps to another channel. Within one drop of blood sometimes 10-20 self assembled mesogen microchips can be seen. If you extrapolate that to the total human blood volume and consider the chips that are being self assembled within the organ systems, the sheer number of potential frequencies emitted from one individual is significant and the mitigation strategies should consider this.

Further articles

Morgellon's filament Chemical Analysis Indicates Organic Polymer That MIT "could not identify" Dr. Staninger 2007

EXPOSURE TO AERIAL EMISSIONS OF NANO COMPOSITE MATERIALS RESULTED IN CHOLINESTERASE INHIBITION - By Toxicologist Dr. Hildy Staninger

Chemical Analysis Of Morgellon's And Chemtrail Fibers - Dr Hildegarde Staninger 2007 - Nano Robots Self Assembling to Nanoarrays, Nanowires - THEY ARE NANOTECHNOLOGY!

Chemical Analysis Of Multiple Morgellon's Fibers From 2007 By Dr. Hildegarde Staninger Sheds Light On Current Advanced Nanomaterials Deployed Against Humanity Via COVID19 Shots And Geoengineering

GLOBAL BRAIN CHIP AND MESOGENS Nano Machines for Ultimate Control of False Memories - Computer System For Collective Mind Control